**Ninth International Conference on Computational Fluid Dynamics (ICCFD9), Istanbul, Turkey, July 11-15, 2016**

**ICCFD9-xxxx**

# Large Eddy Simulations of Heavy Gas Dispersion within Building Group

Weiming Liu[1], Abdullah Alakalabi[1], Tony Graham[1] & Xiaojun Gu[2]

[1]School of Engineering, University of Central Lancashire, Preston, PR1 2HE, UK
[2] Daresbury Laboratory, STFC, Warrington WA4 4AD, UK

Corresponding author: wliu1@uclan.ac.uk

**Abstract:** Heavy or dense gas dispersion within a building group is numerically investigated using the approach of large eddy simulation. The building group is comprised of two kinds of building distributions, collocated and staggered layouts. The numerical results reveal the influence of the building layouts, wind speed, gas leakage source locations to the shapes and concentration distributions of the heavy gas clouds.

*Keywords:* Dispersion of dense or heavy gases, formation of heavy gas cloud, mixing of dense gases and the air, large eddy simulation.

## 1 Introduction

Petroleum gas is a flammable mixture of hydrocarbon gases. It primarily consists of propane and butane. As a fossil fuel, it releases less carbon dioxide and other pollutants per unit energy than do other solid or liquid fuels. Because of this advantage, petroleum gas is increasingly used as a type of energy. Nonetheless, in the transportation, storage and application of petroleum gas, because of various reasons, gas leakage incidents occasionaly happen. When leaked to the atmosphere, the petroleum gas is heavier than the ambient air, which is therefore called dense or heavy gas leakage and dispersion as well. After any leak, the heavy gas will be mixed with the surrounding air to form a combustible gas cloud. The cloud presents a high hazard of fire and explosion and such would produce harmful environmental pollutants. Although various measures to avoid the leakage are put in place, the catastrophes of fire and explosion unfortunately happen from time to time over the world [1]. In order to develop competent technologies to prevent a potential disaster and maintain the safe conditions, it is necessary to study the dispersion of leaked heavy gases and the formation of heavy gas clouds.

The gas leakage can take place in an enclosure or open area. This work is restricted to a study into the gas dispersion in an open area. Traditionally, heavy or dense gas dispersion in an open area is predicted by similarity models [2]. This kind of model assumes a self-similar solution for the concentration of the dense gas species. When the density driving force, i.e., buoyancy, and wind field are specified, the models will predict the dynamic variation of the dense gas cloud shape and hazard extent. Similarity models cannot predict the effects of obstacles.

An alternative to similarity models is computational fluid dynamics (CFD) modeling. The CFD models function by numerically solving the Navier - Stokes equations and can provide very detailed information about the development of the shape of a heavy gas cloud and the hazard extent within very complex geometric spaces. Therefore, a computational fluid dynamics approach is employed to investigate the heavy gas dispersion within a building group in this work.

Turbulence plays a central role in the dense gas mixing and dispersion. When the CFD approach is applied to predict the heavy gas dispersion, numerical simulation of turbulence should be "sufficiently" accurate. At present, a numerical solution for the Reynolds averaged Navier - Stokes (RANS) equations is the primary approach for calculating the turbulence in a complex geometry, for example, the recently published work [3 – 4] used k-epsilon model to calculate the heavy gas dispersion in urban areas. With the advance of CFD technology, large eddy simulation (LES) is becoming more and more popular to simulate the flows in complex geometries. Comparing the two approaches, RANS and LES, we can see that the results produced by LES are more detailed and accurate, but the computational cost of LES is also significantly more than that of RANS approach. The work of this paper presents the results of large eddy simulations of the dispersion of heavy gases within a building group. The open source code, Fire Dynamics Simulator (FDS) [5 – 6], is used in this work. The theoretic base of the solver and settings for the problems in this work are described as follows.

# 2 Basic Equations for Problems

*2.1 Equations of mass, momentum and energy conservations*

The basic equations describing the flow processes satisfy the conservative laws for the mass (1), momentum (2) and energy (3),

$$\frac{\partial \rho}{\partial t} + (u \cdot \nabla)\rho + \rho \nabla \cdot u = 0 \tag{1}$$

$$\rho \frac{\partial u}{\partial t} + \rho (u \cdot \nabla) u + \nabla p = \rho g + \mu \nabla \cdot \{\nabla u + (\nabla u)^T\} \tag{2}$$

$$\rho \frac{\partial e}{\partial t} + \rho (u \cdot \nabla) e + p(\nabla \cdot u) = \nabla \cdot (\lambda \nabla T) + \Phi \tag{3}$$

where $t$ $u$, $\rho$, $T$, $p$, $e$, $\Phi$ and $g$ denote, respectively, the time, velocity vector, density, temperature, pressure, internal energy, dissipation function and gravity vector, while $\lambda$ and $\mu$ are the conduction coefficient and viscosity of the gas mixture, respectively. The term of $(\nabla u)^T$ represents the transpose of $(\nabla u)$. According to the thermodynamics we can obtain the relationship between the temperature and internal energy,

$$e = c_v T \tag{4}$$

where $c_v$ is the specific heat capacity at constant volume.

*2.2 Equations for mass transfer*

It is assumed that the examples studied in this work do not involve chemical reactions; but only the mixing of inert heavy gas with the surrounding air and dispersion. The mixing and dispersion can be described through a set of mass transfer equations for the individual species. Also, the leakage considered in this work is assumed to be gaseous and the mass transfer and flows therefore proceed within a single phase, i.e., gaseous phase only. The basic equations for the mass transfer of the individual gaseous species can be written in

$$\rho \frac{\partial Y_i}{\partial t} + \rho (u \cdot \nabla) Y_i = \nabla \cdot (\rho D_i \nabla Y_i) \tag{5}$$

where $Y_i$ is the fraction of concentration for the species *i* and $D_i$ is its diffusion coefficient. Because of $\sum Y_i = 1$ the continuity equation (1), $\sum [\nabla \cdot (\rho D_i \nabla Y_i)] = 0$ is required.

*2.3 Equations of state*

The equation of state is written as follows,

$$p = \frac{\rho R T}{W} \tag{6}$$

where $R$ is the universal gas constant and $W$ is the local mean molecular mass of the gas mixture which is calculated by

$$W = \sum_i \left( \frac{Y_i}{W_i} \right)^{-1} \tag{7}$$

where $W_i$ is the molecular mass of the species *i*. One can see the molecular mass of the mixture is not a constant. It will vary because of the mixing of the leaked gas with the surrounding air.

The equations (1) – (7) are the basic equations for describing the processes that are studied in this work. Theoretically they are complete and enclosed. With the proper initial and boundary conditions they can uniquely define the processes to be studied. The following section will explain the numerical solutions for these equations.

# 3 Turbulence Models and Numerical Methods

*3.1 Turbulence models*

Turbulence modeling is still one of the most challenging areas of the CFD community at present. In terms of large eddy simulation, the difficulty lies in determining grid Reynolds stresses. The grid Reynolds stresses reflect the effects of the unsolved scale flows to the filtered quantities. They are exactly calculated by a set of integral equations. The computable forms of these integral equations are yet unknown and still an open problem for computational mathematics and physics. In this work, we take the suggestion of Smagorinsky [7] - the Reynolds stresses have the same formulae as the viscous ones, but the turbulent viscosity is calculated by

$$\mu_t = \rho(c_s \Delta)^2 \left[ 2\nabla u : \nabla u - \frac{2}{3} \nabla \cdot u \right] \tag{8}$$

where $\mu_t$ is the turbulent viscosity, $c_s = 0.2$ is an empirical constant and $\Delta$ denotes the length of a grid cell. The symbol ":" denotes the scale product of two tensors.

*3.2 Numerical methods*

The equations (1) - (7) are those for the fully compressible flows. To integrate these equations, the time step width is restricted by the Courant-Friedrichs-Lewy (CFL) number. The velocity in the CFL number for compressible flows are the sum of local sonic speed and flow velocity. Therefore, when the flow velocity is much smaller than the sonic speed which is the case in this work, directly solving (1) - (7) is impractical and filtering acoustic modes from (1) - (7) is necessary [5, 8]. After the acoustic modes are separated from the hydrodynamic modes, the equations to be solved have properties similar to the equations for incompressible flows. As a result, two kinds of problems need to be calculated. One is the Poisson equation and the other is a set of transport equations. Discretization of the Poisson equation results in a system of linear equations that is solved by an elliptic solver FISHPACK [9]. The convective terms in the transport equations are discretized by upwind-biased schemes with the superbee flux limiter [10].

*3.3 Initial and boundary conditions*

The initial conditions include the thermodynamical state and turbulence of the ambient atmospheric environment. In terms of the thermodynamical state, the air is at a temperature of $20\,^{\circ}C$ and at standard atmospheric pressure. The turbulence is produced through the simulation of wind in advance of the gas leakage simulation.

The boundary conditions deal with the flows and mass transfer on physical boundaries. Four types of the boundary conditions are employed. They are inlet, outlet, wall and symmetric boundaries. On the inlet and wall, the flow processes are specified by Dirichlet-type boundary conditions and the mass transfer by a Neumann-type boundary condition, while the flow processes and mass transfer on the outlet and symmetric boundary are all imposed by Neumann-type boundary conditions. Which of the boundary conditions is applied depends upon the concrete case study and will be described in the following sections in detail.

# 4 Validation of Numerical Simulations

Before representation of the results, let us compare a numerical simulation produced by the models mentioned above with the experimental measurements for the gas dispersions over a solid obstacle. The experimental measurements carried out by Ayrault et al [11] in the EDF-ECL atmospheric wind-tunnel. A point source for gas release is placed at 400 mm ahead of a thin solid fence or obstacle. The fence thickness is so thin as to be neglected while its heights are 30 mm and 60 mm for the two experimental setups, respectively. Two kinds of gases, dense gas with the molecular mass of 58.12 and neutral gas with the same molecular mass as the ambient air, are released from the source. The released gases disperse caused by two forces, the buoyancy produced by the difference between the released gas densities and ambient air density and wind flow with a speed of 1 m/s. The dispersions of the released gases were experimentally measured and reported in the paper.

The numerical modelling is set up with the same configuration as the experiments. The computational domain has a dimension of $2m \times 3m \times 0.32m$ in x, y, and z coordinate axes, respectively. The computational domain is meshed with cells of $2.5mm \times 2mm \times 2mm$. On the x-z plane cross the minimal y coordinate, the inlet boundary conditions for the wind with the speed profile same as the experimental are specified, while the outlet boundary conditions are posed on the x-z plane cross the maximal y coordinate. The ground and surfaces of the solid obstacle are taken as no-slip boundaries. On the other boundaries of the domain symmetric boundary conditions are imposed. The computations start with uniform initial conditions and integrate the processes up to 300 sec.

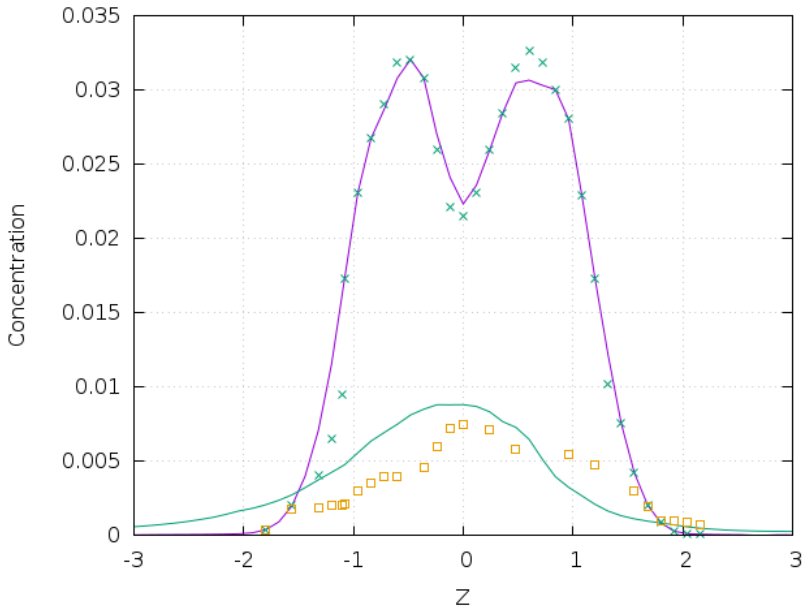


(a)

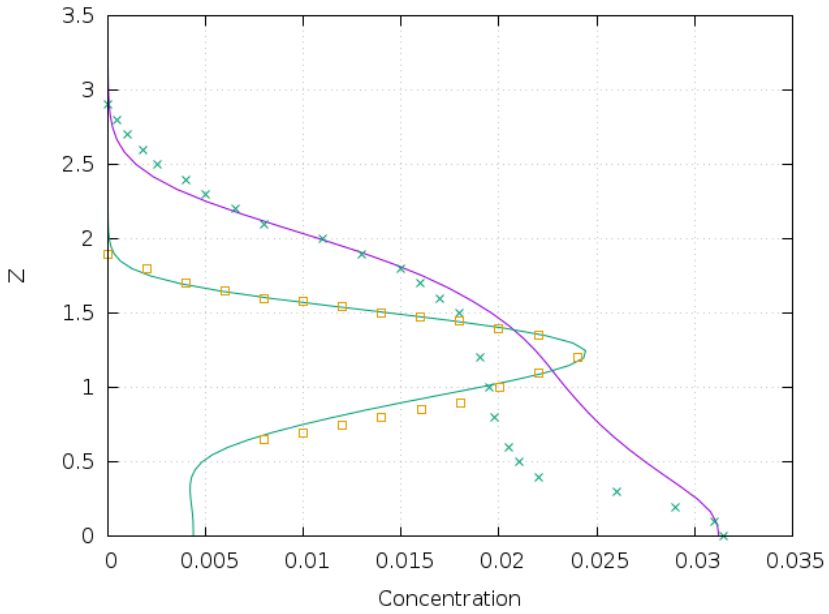


(b)

Figure 1 comparison of the numerical simulations and experimental measurements [11] for the concentration profiles on horizontal (a) and vertical (b) sections at 200 mm behind the obstacle. The purple curves are for the heavy gas dispersion, green ones for the neutral gas dispersion and empty points and cross points for the experimental results. The concentration is normalized by a reference concentration (mean concentration at the release source)

The gas dispersions produced by the numerical simulations are consistent with the experimental observations of [11]. Nonetheless, because of errors of experiments and of numerical simulations, some differences between the experimental and numerical results. Figure 1 is a typical case that shows the comparison of the numerical simulations and experimental measurements for the concentration profiles on horizontal and vertical sections positioned 200 mm behind the obstacle. One can see a significant difference between the heavy gas dispersion and neutral gas dispersion. The difference is caused by the buoyancy produced by the distinct densities of the gases. First of all, the flow in the heavy gas dispersion presents a pattern of double bubbles, but the flow in the neutral gas dispersion has only one bubble. This result is in agreement with other experimental observations [12] as well. In order to visualise the flow patterns in detail, a comparison of the two structures is displayed in figure 2, which indicates the concentrations of the gases on sections located 50 mm above the ground. It should be pointed out that the concentration profile for the neutral gas dispersion in figure 1 (a), produced by the numerical simulations, is symmetric, but the experimental data expresses some deviation. The deviation is presumably produced by the measurement errors.

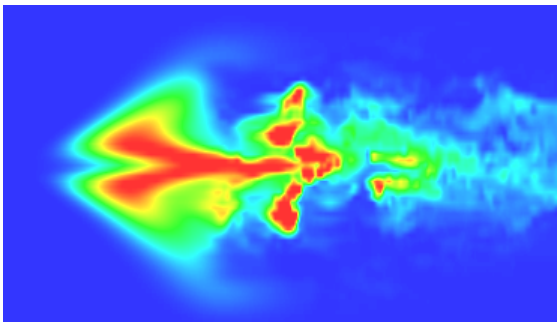

(a)

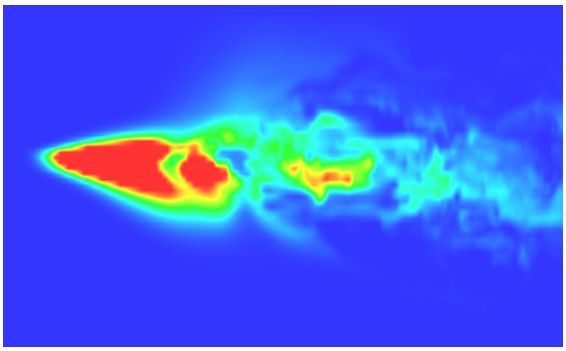

(b)

Figure 2 concentrations of the heavy gas (a) and neutral gas (b) on the section of 50 mm above the ground in which the red indicates the maximal concentration and the blue shows zero concentration, i.e., it is normalized by the maximal concentration, the red colour is for one and the blue for zero.

The second significant difference is in the effect of obstacle on the gas dispersion, which can be observed in figure 1 (b). For the heavy gas, the maximum concentration is at the ground, but the maximum concentration of the neutral gas is above the obstacle. This conclusion shows that the solid block is not an effective measure to resist the heavy gas dispersing to the ground level. Comparing the results produced numerically and experimentally, we can see both are quite identical for the neutral gas dispersion. For the heavy gas dispersion, however, the concentration around the top edge of the obstacle is over-predicted. This could reflect some inaccuracy of the numerical models and methods mentioned above.

# 5 Results and Discussions

Now we move on to present the results of heavy gas dispersion within buildings. The gas release source in this work is a point source with a constant flow rate of $0.05 m^3 s^{-1}$ and the gas is butane. The location of the gas release source, such as the height and plane position, has a significant influence on the heavy cloud formed. In this work, the sources are on the ground, but they can be placed in different positions within the buildings. The details of the gas release sources will be given in each case study. Moreover, the temperatures of the released gases and ambient air are assumed to be same. Hence, the mixing and dispersion of the gases are driven by wind turbulence and buoyancy produced by the density difference between the heavy gases and air.

In order to obtain accurate results with the available computational resource, the numerical simulation in this work is a small-scale and building-simplified model. The building is assumed to be of cuboid shape and its dimension is $1m \times 1m \times 2m$, here 2m is its height. The simulation domain is a cuboid with dimension of $22m \times 44.8m \times 6.4m$, in which about 150 buildings are embedded. The buildings are distributed by two kinds of manners inside the computational domain, collocated and staggered layouts. The distance between two buildings is 1 m. The domain is meshed non-uniformly. The area immediately surrounding the buildings is meshed with fine elements and the spaces further away from buildings with a coarse mesh. The fine elements have a length of 0.05 m. In all, the number of elements was kept under 20 million. On the left hand side of the domain, a wind inlet boundary condition was specified and on the right hand side was an outlet boundary. The bottom of the domain is the ground, on which a solid surface boundary condition is imposed. On the other sides of the domain, symmetric boundary conditions were applied. The simulation started with uniform initial conditions and integration proceeded up to 3600 sec. However, the numerical results show that the processes have already become stationary at 600 sec.

Atmospheric turbulence is produced by the atmospheric wind flow that is exerted on the inlet boundary. The atmospheric wind profile is assumed to be of the form, $u_0 (z/z_0)^n$, here $z_0$ is the height of the atmospheric boundary layer and $u_0$ is the wind speed at $z_0$, $n$ is an index of the power

profile. In this work, we assume $u_0 = 0.75m/s$, $z_0 = 100m$ and $n = 0.15$.

*5.1 Collocated distribution of the buildings*

The source of gas release is at the left edge of the building of row 6 and column 4, see figure 3. After a transient from the beginning of the simulation, the process approaches to a quasi-steady state. The transient development takes about 60 sec – 100 sec. By the quasi-steady state, the shape of the heavy gas cloud and its concentrations are fixed on average, although the detailed course is still unsteady because of turbulence. Figure 3 displays the concentrations on four horizontal cross-sections parallel with the ground. From the figures one can image the shape of the gas cloud. Downstream it looks like a prism and upstream like an elliptic-cylinder. However, the values of concentration decrease with increasing height. At a level of 1 m from the ground, that is, the level of a half building height, the concentrations are very small and almost zero. Two factors, wind and buildings, influence the shape of the formed gas cloud. The wind leads to asymmetry of the shape between the downstream and upstream parts. The stronger the wind the more flat the elliptic-cylinder and the longer the tail of the prism. The numerical results also show that the building layout is the direct reason for the prism shape of the gas cloud. This result is basically consistent with the experimental observation obtained by Heidorn et al [13].

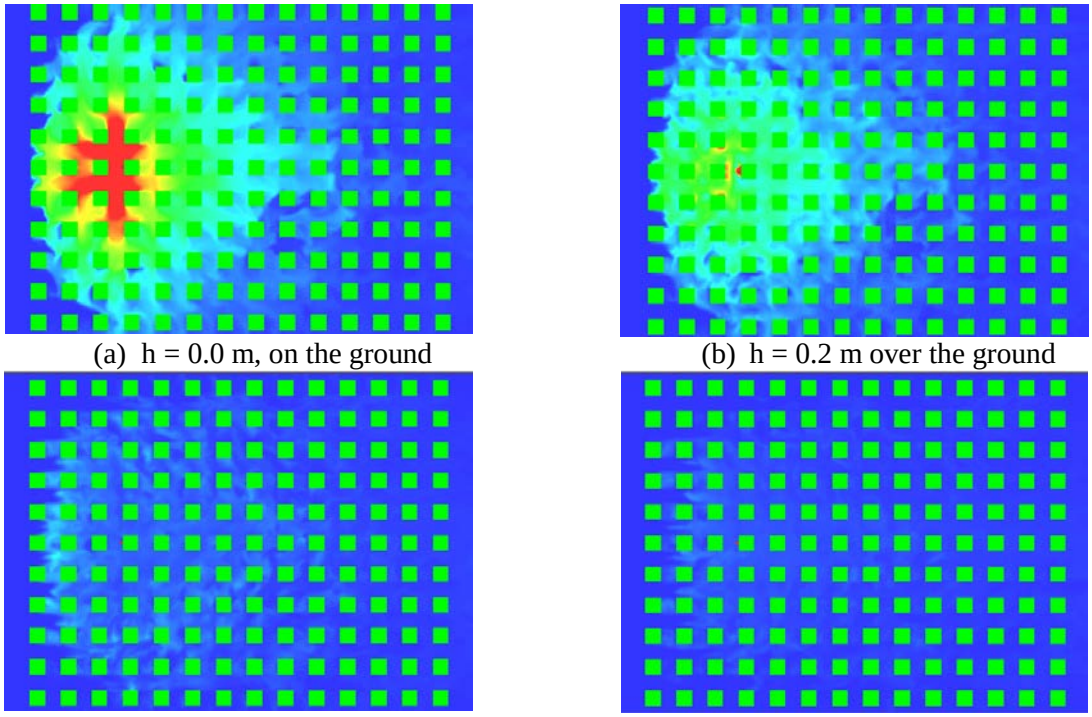

(a) h = 0.0 m, on the ground (b) h = 0.2 m over the ground

(c) h = 0.5 m over the ground (d) h = 1.0 m over the ground

Figure 3 concentrations of heavy gas for the collocated distribution of buildings, in which the release source is ahead of the building of row 6 and column 4 and the colour red indicates the concentration of 0.01 mol/mol and blue is for the concentration of zero.

Two forces drive the processes of the heavy gas dispersion and mixing. One is wind-force and the other is buoyancy. The wind-force can be measured by wind speed, i.e., wind momentum, while the buoyance is directly related to the local density of the mixture of the heavy gas and ambient air. The mixture density is determined by the local thermodynamic state and concentration of the heavy gas. In this work, we assume that the process is isothermal and therefore only the concentrations of the heavy gas cause the buoyancy. The concentrations of the gas, however, have been mentioned above. Now we therefore move on to have a look at the wind speed. Figure 4 visualizes the flow velocity vectors on three horizontal cross-sections. In the figure wind blows from the left hand side to the right hand side. Within the buildings, one can see that various complex vertexes are produced. Firstly, the heavy gas is released from the source. Then it is driven by these vertexes to be mixed quickly with the

neighboring mixture and is subsequently dispersed away from the source. Finally the gas dispersion forms a quasi-steady heavy gas cloud. This heavy gas cloud generates a zone of major hazard. If the expanding zone meets a hot-temperature source, a terrible explosion and fire could take place. Even if no explosion or fire occur, the highly contaminated environment inside the zone will have a negative impact upon human health.

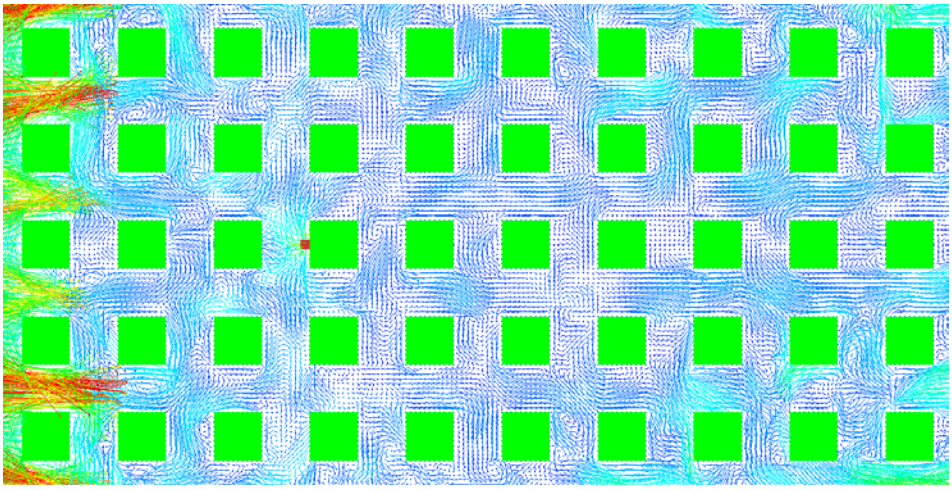

(a) h = 0.2 m over the ground

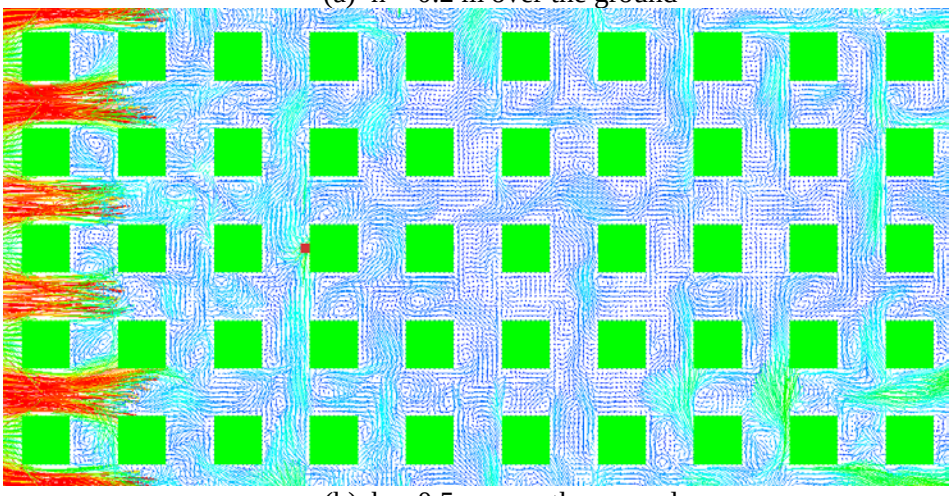

(b) h = 0.5 m over the ground

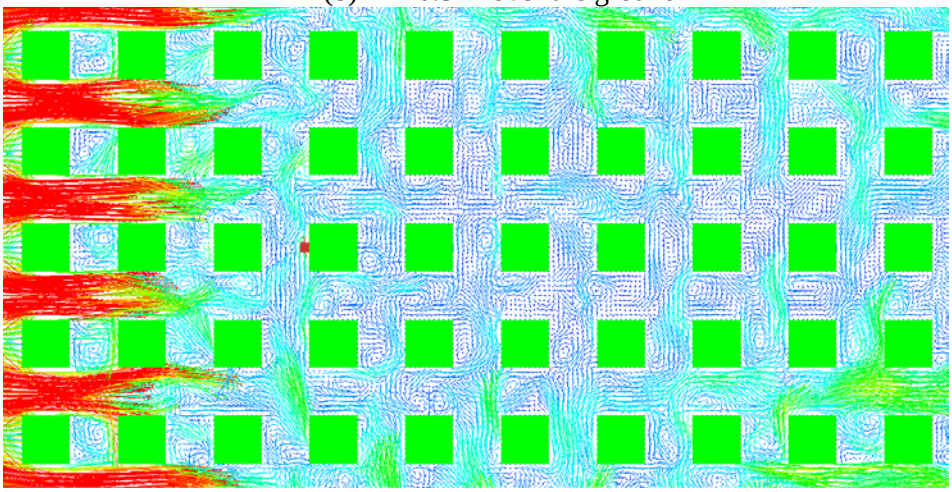

(c) h = 1.0 m over the ground

Figure 4 velocity vectors for the collocated distribution of buildings, in which the colour red indicates the velocity of 0.25 m/s and blue is for the velocity of zero.

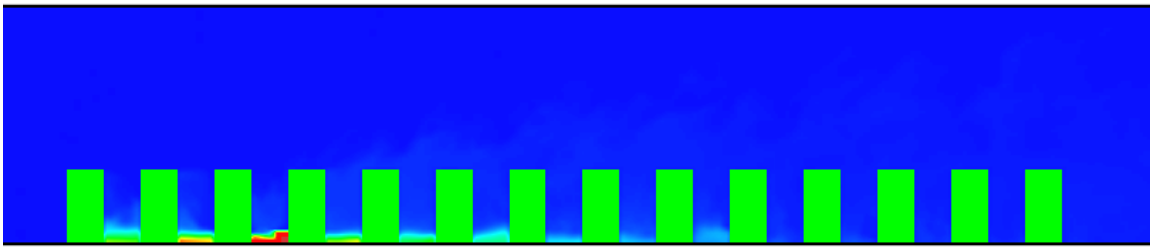

(a) concentrations of release gas

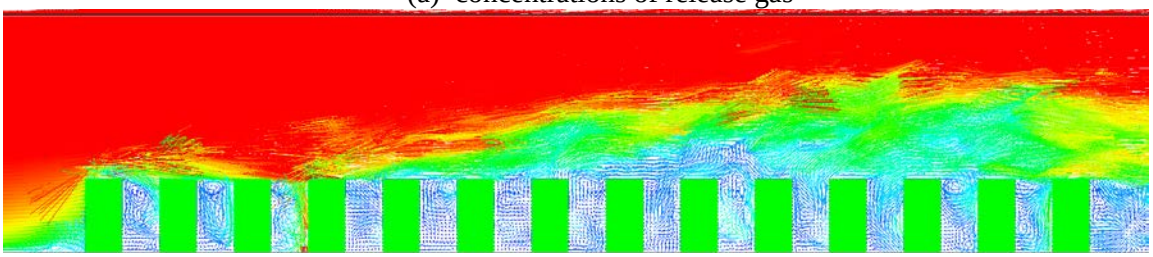

(b) velocity vectors

Figure 5 concentrations and velocity vectors on vertical section for the collocated distribution of buildings.

In order to have a complete picture about the gas cloud, the concentrations and flow velocity vectors are illustrated in vertical cross-section on figure 5 as well, from which it is observed that the heavy gas tends to flow over the ground, but the vertical eddies of turbulence drive the gas to spread vertically which enhances the height of the gas cloud.

Figure 6 shows the profiles of the concentrations of the released gas. In the figure, the distances of x and y are measured from the release source. Associated with the building dimension, figure 6 actually gives the quantitative relationship of the concentrations against the geometric dimension of the heavy gas cloud. The closer to the source the higher the concentration. At a distance of 2 m, i.e., two times of building width, away from the source, the concentration value will decrease about 50%. Further away from the source, however, the reduction will become flat. The profiles across the wind direction, see figure 6 (b), indicates a symmetric pattern, while ones along the wind direction, see figure 6 (a), are non-symmetric, as the wind makes an effect. In the figure there is the appearance of multiple peaks in the profiles. These peaks are produced by the spaces between buildings and indicate the hot-spots are there.

In order to study the effect of gas release source locations, a scenario was modelled with the gas release source in the canyon between the building row 5 and 6, that is, the gas release source in the above case study was moved 1 m in parallel from the edge of the building to the canyon centre. The numerical results (figure 7) show that the length of the heavy gas cloud across the wind direction is reduced compared with the case of the source at the building edge, but the length along the wind direction increases. For example, figure 7 shows a comparison of the concentrations on the ground produced by both case studies. This is because the released gas from the canyon source has less resistance along the wind direction. As a result, the gas cloud is of longer size in that direction.

### *5.2 Staggered distribution of the buildings*

This is another typical case. The results from this case study produced the effects of the building layout on the heavy gas dispersion. Similarly to the case study in section 5.1, three positions of the release sources were explored. One position was at the upwind front of the building, one was at the downwind rear behind the building and the third one was placed in the middle between the first position and second position. In contrast to the case study in section 5.1, the numerical results for the staggered distribution of the buildings show that variation of the release source positions produces little influence to the heavy gas dispersion and cloud shape. Therefore, the case with the third release source is used for the following discussion.

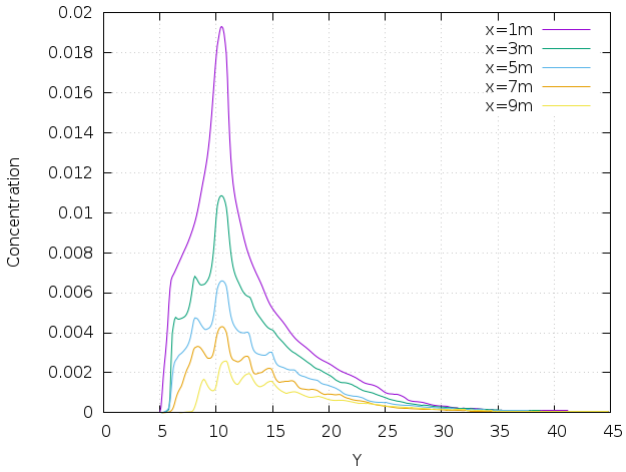


(a) along the wind direction

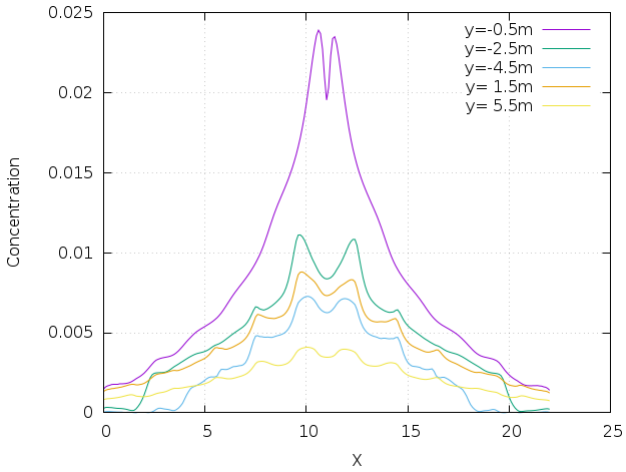


(b) across the wind direction

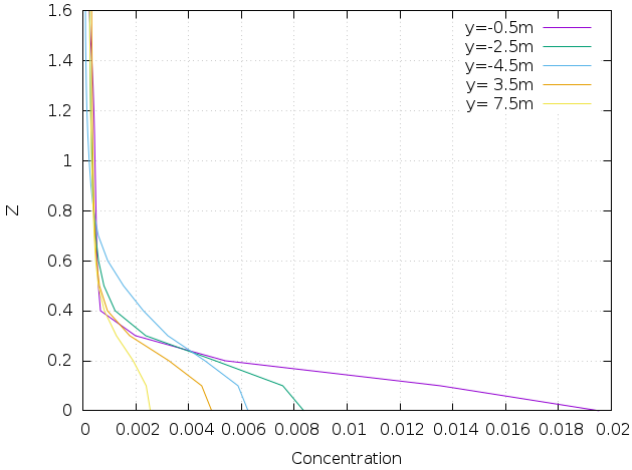


(c) vertical direction

Figure 6 profiles of concentrations for the collocated distribution of buildings in which the distances of x and y are measured from the release source.

Concentrations and flow velocity vectors on horizontal cross-sections for this case study are visualized in figure 8. This figure shows the basic features of the heavy gas cloud. One can see that the shape of the gas cloud in this case study is significantly different from those in section 5.1. The upstream part of the gas cloud shape for the staggered distribution of the buildings becomes flatter

and also the width of the shape increases when compared with the gas cloud shapes for the collocated distribution of the buildings in section 5.1. The reason for this can be found from the flow velocity vectors, see figure 4 (a) and figure 8 (b). When comparing both vector pictures it can be found that the flow velocity vectors in figure 8 (b) form a virtual "wall" in the buildings of column 2 which blocks the gas dispersion upstream. The blocked gas with higher concentrations enhances its spread in the cross-wind direction and makes the gas cloud wider.

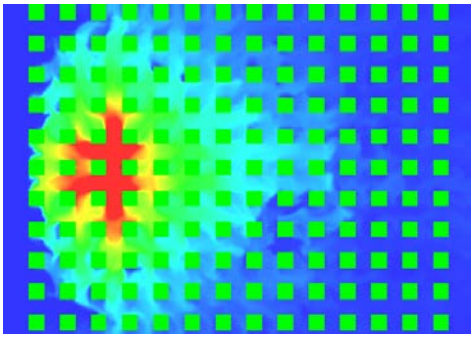

(d) ahead of the building

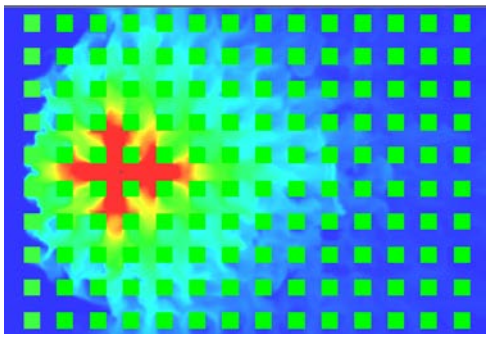

(e) in the side of the building

Figure 7 comparison of concentrations produced by two different locations of the sources, (a) ahead of the building and (b) in the side of the building

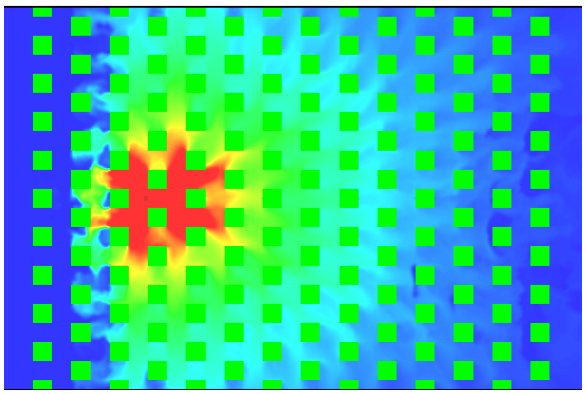

(a) concentrations of release gas

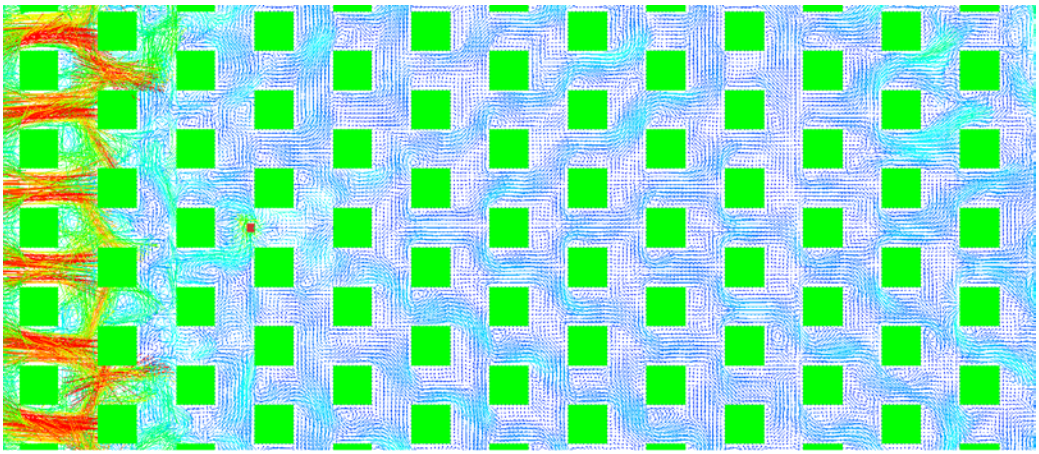

(b) velocity vectors

Figure 8 concentrations and velocity vectors on vertical section for the staggered distribution of buildings: the concentrations are on the ground and the velocity vectors are on the section of 0.2m from the ground.

*5.3 Comparison of numerical simulations and experimental observations*

The experiment was done by Heidorn et al [13]. Before this comparison it should be noted that there are two differences between the numerical simulations and experiments. The first is that the gas dispersion in the numerical simulations is affected by a simulated wind with constant speed 0.75 m/s but the experimental data were obtained without wind. The second is that the gas in the numerical simulations is continuously released from the source but the experimental gas release source was instantaneous, i.e., a volume of gas was stored in a cylinder and when the experiments start the cylinder was suddenly removed and the gas mass was free to disperse. Although the two differences exist, the comparison as follows yet gives the similarity of the basic features of the results produced by both.

Figure 9 illustrates the concentrations of the heavy gas for the experiments and numerical simulations. The numerical results are those for the cross-section of 0.2 m from the ground. It is found that the shapes of the heavy gas cloud for the numerical calculations and experiments are similar in the downstream part, but the upstream part had significant differences. As the wind acted on the gas dispersion in the numerical simulations, the upstream part of the gas cloud shape produced by the numerical simulations was more flat than that seen in the experiment. In the cross-wind direction, however, the numerical results are quite in agreement with the experimental visualizations.

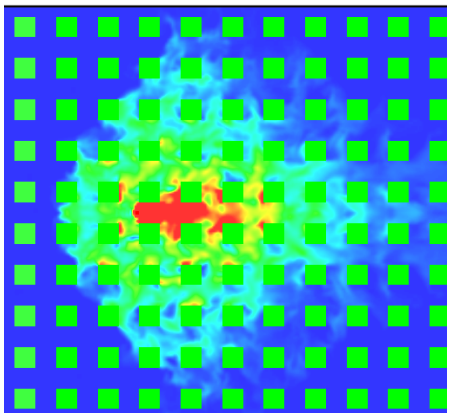

(a) concentrations of numerical simulation for collocated distribution of the buildings

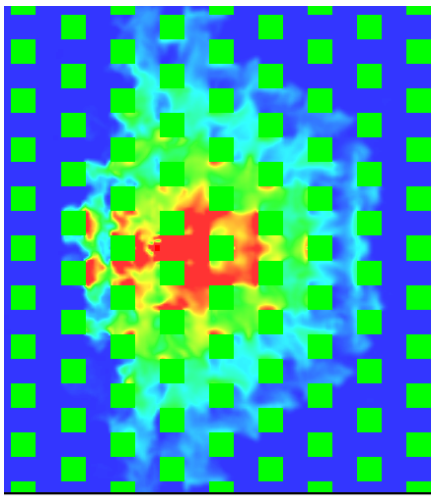

(b) concentrations of numerical simulation for staggered distribution of the buildings

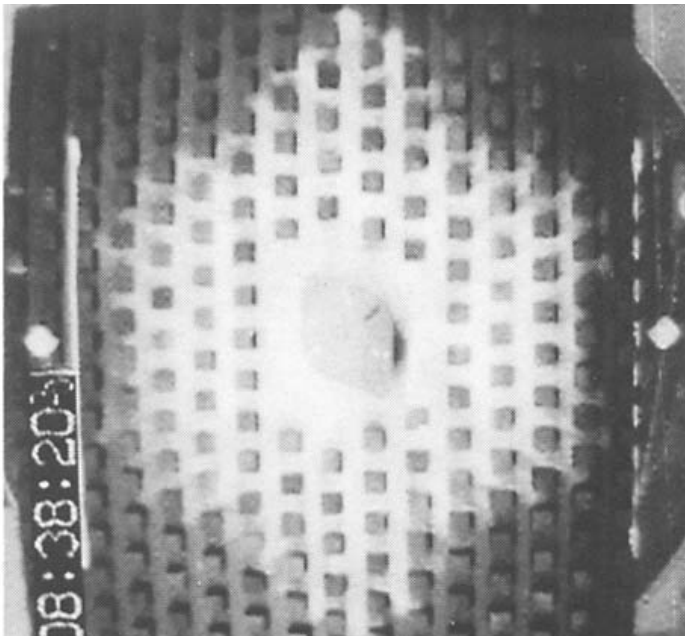

(c) concentrations of experiments from [13]

Figure 9 comparison of concentrations produced by numerical simulations and experiments

# 6 Conclusions

Two typical scenarios of heavy gas leakages were simulated using the large eddy simulation approach, one with a regular distribution of about 150 buildings and the other with a staggered distribution of the buildings. Before simulating the scenarios, a comparison of the numerical simulations with experimental observations were done, which shows the gas dispersions produced by the approach used in this work are basically of agreement with the experiments. In addition, the numerical simulations for the two scenarios produce similar patterns and shapes of the heavy dispersions to the existing experimental data. All of these show that the numerical results produced in this work are reasonably accurate and reliable.

The numerical simulations produce a very useful data base for the applications such as detection, installation and risk assessment and management. Nonetheless, when exploring the numerical results it was found that the building layouts have significant influences to the formation of gas clouds. This reflects the complexity of the problem and high sensitivity of the processes to the external conditions. Further development of the data base for various case studies will be necessary and useful for hazard management and control. The future work for this topic will focus on the risk assessment with the produced dense gas clouds, which is involved in explosions and fires caused by them.

# References


[1] The 100 Largest Losses 1974 - 2013, 23rd Edition, Marsh & McLennan, 2014

[2] Witlox, H, The HEGADAS model for ground-level heavy gas dispersion – I, steady state model, Atmosperic Environment, 28:2917 - 2932, 1994

[3] Pontigga, M, Derudi, M, Alba, M, Scaioni, M, and Rota, R., Hazardous gas releases in urban areas: assessment of consequences through CFD modelling, Journal of Hazardous Materials, 176:589 – 596, 2010

[4] Scargiali, F, Grisafi, F, Busciglio, A. and Brucato, A, Modelling and simulation of dense cloud dispersion in urban areas by means of computational fluid dynamics, Journal of Hazardous Materials, 197:258 – 293, 2011

[5] McGrattan, K, Baum, H. and Rehm, R, Fire-driven flows in enclosures, Journal of Computational Physics, 110:285–291, 1994

[6] McGrattan, K, Hostikka, S, Floyd, J, Baum, H. and Rehm, R, Fire dynamics simulator (version

5) technical reference guide, NIST Special Publication, 1018 – 5, 2007
[7] Smagorinsky, J, General Circulation Experiments with the Primitive Equations I the basic experiment, Monthly Weather Review, 91(3):99–164, 1963
[8] Liu, W, Makhviladze, G, An implicit finite element solution of thermal flows at low Mach number, Journal of Computational Physics, 227:2743 – 2757, 2008
[9] Adams, J C, Swarztrauber, P N and Sweet, R, FISHPACK - Efficient FORTRAN subprograms for the solution of separable elliptic partial differential equations, https://www2.cisl.ucar.edu/resources/legacy/fishpack
[10] Leveque, R J, Finite volume methods for hyperbolic problem, Cambridge University Press, Cambridge, UK, 2002
[11] Ayrault, M, Simoens, S and Mejean, P, Negative buoyancy effects on the dispersion of continuous gas plumes downwind solid obstacles, Journal of Hazardous Materials, 57:79 – 103, 1998
[12] Hall, D J and Walters, R A, investigation of two features of continuously released heavy gas plumes, Warren Spring Laboratory Report, LR 707, 1989
[13] Heidorn, K C, Murphy, M C, Irwin, P A, Sahota, H, Misra, P K and Bloxam, R, Effects of obstales on the spread of a heavy gas – wind tunnel simulations, Journal of Hazardous Materials, 30:161-194, 1992.